Nano Today (2010) 5, 175—182

available at www.sciencedirect.com

ScienceDirect

journal homepage: www.elsevier.com/locate/nanotoday

RAPID COMMUNICATION

External electric field driven 3D ordering architecture of silver (I) oxide meso-superstructures

Jixiang Fang[a,b,*], Philipp M. Leufke[a], Robert Kruk[a], Di Wang[a], Torsten Scherer[a], Horst Hahn[a]

[a] *Karlsruhe Institute of Technology (KIT), Institute für Nanotechnology, 76021 Karlsruhe, Germany*
[b] *School of Science, Xi'an Jiaotong University, Shann Xi, 710049, People's Republic of China*

Received 10 February 2010; received in revised form 11 April 2010; accepted 3 May 2010

KEYWORDS
Meso-superstructures;
External electric field;
Ordering assembly;
Polyhedral Ag_2O

Summary We report an external electric field driven particle-mediated ''bottom-up'' assembling methodology to in situ build the Ag_2O meso-superstructures with controlled shape and size within an electrochemical deposition system. Different shapes (rhombic hexahedron, cube and dodecahedron) and sizes (around 100 to ~800 nm) of Ag_2O mesocrystals have been obtained by the adjustment of the applied overpotential as well as the growth time. Various overpotentials play a crucial role in determining the shapes, structures as well as growth modes of the final product. The growth mechanism of polyhedral structures of Ag_2O meso-superstructures is explained by the oriented attachment from the nature of crystallographic surfaces and the external electric induced ordering alignment process of primary nanoparticle building blocks. Thus, the current strategy not only provides the direct evidence of an external electric field driving in situ mesoassembling process, but also may be extended to other systems to synthesize the meso-superstructures.

Introduction

Recently, a new growth mechanism, i.e. the non-classical crystallization pathway was successfully elucidated by Cölfen et al. for the minerals grown by biomineralization processes [1,2]. This particle-by-particle growth process always involves the oriented attachment [3,4] or grain rotation [5] of the building units and forms the so-called mesocrystals via the mesoscale transformation [6]. Mesocrystals are colloidal crystals composed of individual nanocrystals that are aligned in a common crystallographic fashion, exhibiting scattering properties similar to a single crystal [7]. With the appearance of the mesocrystal concept, attention has been directed towards the investigation in various systems. The mesoscale transformation process seems to be relevant in many cases: for exam-

* Corresponding author. Tel.: +49 7247 82 8313; fax: +49 7247 82 6368.
E-mail addresses: Jixiang.Fang@kit.edu, jxfang@mailst.xjtu.edu.cn (J. Fang).

1748-0132/$ — see front matter © 2010 Elsevier Ltd. All rights reserved.
doi:10.1016/j.nantod.2010.05.002

ple, Cu_2O [8], ZnO [9], NH_4TiOF_3/TiO_2 [10], PdS [11], ZnSe [12], calcium carbonate [13], even in pure metals, Au [14] and Ag [15—17]. The resulted mesocrystals were characterized by notable internal porosity, small size of their building blocks (around 10 nm scales) as well as the rough surface. Materials with such features are ideally suited to many applications, such as catalysts, sensors and optical properties. However, up to now, some basic fundamental aspects, such as the underlying growth mechanism during the mesoscale transformation, methods to intentionally employ this unique growth mode to artificially synthesize a variety of materials in a controlled way, and the novel properties of these unusual meso-superstructures (compared to the perfect single crystal or polycrystalline structure with the same chemical composition), remain largely unexplored.

The intrinsic properties of a material are mainly determined by its size, shape, composition, crystallinity, and structure. Herein, tailoring the architecture of nanocrystals has attracted great interest in past decades due to the unique shape and size-dependent effect. Previous strategies to control the growth of anisotropic nanostructures have always involved either hard templates or softer directing agents, including surfactants or polymers [18]. Although good control over the dimensions can be realized in these syntheses, removal of the template or directing agent from the surface of the product require harsh conditions or multiple washing. More important, the residue of surfactants or polymers on the product surface may cause significant problems in some applications, such as surface-enhanced Raman scattering that gives vibrational information on molecules adsorbed on the surfaces of nanomaterials. Therefore, controlled synthesis of various nanostructures with surfaces as ''clean'' as possible is still challenging.

Silver (I) oxide (Ag_2O), a *p*-type semiconducting oxide, has been used mainly in thin film sensors and as a cathode in zinc—silver oxide batteries [19,20]. The bandgap of Ag_2O, which has the same crystallographic structure as Cu_2O [4], has been determined experimentally to be of 1.3 ± 0.3 eV. This indicates that Ag_2O, being nontoxic, is potentially suitable for an ideal light absorption layer in photovoltaic cells (PVs). For the above applications, a shape tailoring which determines the surface atomic arrangement and coordination represents is of important. To date, Ag_2O nanoparticles or thin films with different structures have been synthesized by various routes [21—23]. However, to our knowledge there are no reports on the polyhedral structures of Ag_2O, such as cubes or dodecahedrons, although these nanostructures have been synthesized in other systems, such as Cu_2O, CeO_2, PbS, PbSe, FeCo, BaF_2, CaF_2, or even in pure metals, like Pd, Ag, and Cu [24—27].

In order to artificially synthesize the mesocrystals in a wide class of materials, the formation mechanisms need to be elucidated. In fact, our previous studies upon the synthesis of Ag mesocrystals [16] as well as the crystal growth in gels [2] have implied that a high supersaturation and high particle nucleation rate (forming abundant small clusters—the building blocks for the mesocrystals) preferentially induces mesocrystal formation rather than the ion-mediated classical crystallization process [2]. On the other hand, recent literature examples, for the system of slow evaporation of the solvent, indicate that the ordering physical fields/forces like electric, magnetic, or dipole fields, can be also important to allow for an ordering of the nanoparticle units [28—31]. More recently, Cölfen et al. have predicted an external electric field would play an important role in the formation of highly ordered nanoparticle superstructures [32]. To date, the relevant experimental investigation is still unavailable.

Here, we present the first evidence how an external electric field influences on the in situ construct Ag_2O meso-superstructures with controlled shapes, sizes and structures. An electrodeposition process with an extremely high overpotential which provides either a redox environment or an external electric field is employed to synthesize the Ag_2O mesocrystals with controllable polyhedral structures. Various applied overpotentials result in a series of different shapes of Ag_2O mesocrystals, such as rhombic hexahedrons, cubes, and dodecahedrons. In particular, the investigations of the early stages of the architectural process give deeper insights into the growth mechanism in the present electrochemical synthesis system. Due to no surfactants or polymers are used in the reaction, therefore, a clean surface is obtained which is critical in some applications, such as sensors, catalysts, as well as surface-enhanced Raman scattering (SERS).

Experimental section

Synthesis of Ag_2O meso-superstructures. All chemicals were used as-received without further purification. Typically, the electrolyte solution is prepared with analytical reagent $AgNO_3$ (Chempur, purity: 99.99%) and ultrapure water. The electrodeposition is conducted in a double-electrode system, where two parallel silver plates (99.995%) with dimension $5\,mm \times 5\,mm \times 0.5\,mm$ are separated by a distance of 3 cm so as to minimize the influence from distance change between anode and cathode during deposition of cathode. To test the idea of mesoscale assembling of Ag_2O mesocrystals via an extremely high overpotential, a strong direct current (DC) potential with range of 1—60 V is applied between two silver plates electrodes during electrochemical deposition. As electric current passes between the two electrodes, the brown-colored dispersed Ag_2O deposits can emerge in the vicinity of the anode and fall off into the solutions. The silver plates of anode are directly used for the observations of SEM, and the brown deposits are collected onto a $1\,cm \times 1\,cm$ silicon substrate for further investigations.

The specimens synthesized under different electrochemical reaction conditions are selected for characterization by X-ray diffraction (XRD), scanning electron micrographs (SEM), X-ray photoelectron spectroscopy (XPS) and transmission electron microscopy (TEM). The TEM observations were performed with a FEI-Titan 80—300 operated at 300 kV. The TEM samples were prepared by carefully removing the product from the Si substrate onto a carbon-coated TEM grid. The XRD data were collected using a Philips X'PERT diffractometer via Mo Ka radiation. The general morphology of the products was characterized by FESEM (LEO 1530). XPS measurements were conducted by use of a Specs Phoibos 150 electron spectrometer and Al and Mg Kα radiation.

Table 1 Binding energy for Ag 3d and O 1s photoelectrons for electrodeposited Ag_2O mesostructures.

Sample	Binding energy (eV)[a]	
	Ag $3d_{5/2}$	O 1s
Ag_2O mesostructure	368.0	531.7
Si substrate		532.5
Ag[b]	368.3	
Ag_2O[b]	367.9	529.4
AgO[b]	367.5	528.7, 531.6

[a] XPS analysis was performed with Al and Mg Kα radiation at a pressure of $\sim 1.5 \times 10^{-8}$ Pa.
[b] Literature values cited in this paper by Ida et al. [21].

Results and discussion

The Ag_2O mesocrystals were synthesized in $AgNO_3$ (aq.) using a simple two-electrode system reported in our previous paper [33]. Only three ingredients are required in this protocol: silver nitrate, water and silver electrodes. The silver anode serves as the metal (ion) source to provide silver ions in the electrolyte solution during the progress of the electrochemical reactions. As electric current passes between the two electrodes, white-colored silver tresses grow from the cathode, while brown-colored dispersed Ag_2O deposits can also emerge in the vicinity of the anode via an anodic oxidation process [34] and fall off into the solution. These brown deposits are collected onto a 1 cm × 1 cm silicon substrate for further investigations. The chemical composition of product is characterized using XPS and XRD. Electronic states of the Ag_2O deposits were examined on Ag 3d and O 1s by XPS analysis (Table 1, and see the Supporting Information Fig. S1). Ag $3d_{5/2}$ and O 1s peaks were observed at binding energies of 368.0 and 531.7 eV, respectively. These values agree well with those for Ag_2O in the literature [21]. The XRD patterns of the resultant deposits are presented in Fig. 1. All diffraction peaks could be assigned to either Si substrate or Ag_2O with a cubic cuprite structure (JCPDS 76-1393). A comparison with the JCPDS data indicates that the electrodeposited Ag_2O has a ⟨1 0 0⟩-preferred growth orientation, particularly in the shapes of rhombic heaxahedron and cube. The lattice constant of the Ag_2O was calculated to be 4.718 Å from the XRD pattern, which is consistent with the JCPDS data, 4.72 Å.

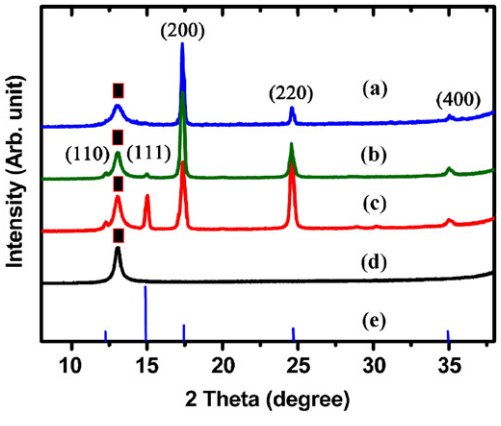

Figure 1 XRD patterns of Ag_2O mesocrystals synthesized at silver ion concentrations of 1 mM, applied potential and growth time of (a) rhombic hexahedron, 30 V @ 3 min, (b) cube, 15 V @ 3 min and (c) dodecahedron, 5 V @ 5 min, (d) Si substrate and (e) JCPDS data (76-1393) for Ag_2O.

In this study, various concentrations of silver ions, applied potentials (1—60 V) as well as different growth times were investigated to synthesize Ag_2O mesostructures of various shapes and size. Fig. 2 shows the field emission scanning electron micrographs (FESEM) of three polyhedral structures of Ag_2O mesocrystals synthesized at the silver ion concentrations of 1.0 mM and applied potential of (a) 30 V, (b) 15 V, and (c) 5 V. With 30 V of the applied potential and 3 min of the growth time, the products shape is of rhombic hexahedron bounded by {1 0 0} faces with an edge length of about 200 nm (Fig. 2a). The shape of rhombic hexahedron is also confirmed by the XRD patterns recorded from the Ag_2O mesocrystals on the silicon wafer (Fig. 1), where the exceptionally strong (2 0 0) diffraction peak for the rhombic hexahedron indicates that the {1 0 0} surfaces of the Ag_2O mesocrystals are preferentially parallel to the substrate. When the applied potential decreases to 15 V, the mesocrystals assume a form of relatively uniform cubes enclosed by {1 0 0} planes (Fig. 2b). With the 3 min growth time, the Ag_2O cubes display a mean size of approximately 150 nm. As the further reduction of the applied potential to 5 V, the typical shape of the product transforms into rhombic dodecahedral enclosed by {1 1 0} planes (Fig. 2c). The size is about 200 nm for the growth time of 5 min. The XRD patterns for above different products give the signature upon the structural transformation of Ag_2O mesocrystals. It should be noted that these mesocrystals consist of a large quantity of nanoparticles of the approximately 10 nm size (the magnified images in the insets of Fig. 2a—c). The rough surfaces of the polyhedral Ag_2O strongly suggest a change of crystallization mechanism from the classical ion-by-ion growth to the non-classical mesoscale assembly or mesocrystallization [1,6,9].

High-resolution transmission electron microscopy (HRTEM) and the selected area electron diffraction (SAED) pattern provide further insight into the mesocrystallization mechanism of the polyhedral Ag_2O mesocrystals. Fig. 3a shows a typical bright-field TEM image of individual Ag_2O mesocube with the size of approximately 200 nm. Clearly, the bright—dark contrastive spots in the TEM image indicate that the Ag_2O cube is aggregated by a number of small primary nanocrystals (the building units of mesoscale assembly) with sizes of 10—15 nm. The single crystal-like pattern consisting of individual diffraction spots (Fig. 3b) indicates that the whole assembly of the building units is highly oriented and aligned. A few isolated symmetrical spots in the diffraction pattern also suggest that there is a narrow range of small angle lattice mismatch between the boundaries of the nanoparticles when assembling in the same orientation. This is a typical situation during the processes of mesoscale transformation for mesocrystals [1,6,9]. The HRTEM image (Fig. 3c) taken from the dashed white circle area of Fig. 3a further supports the claim of analogous single crystallinity, where the primary nanoparticles shares the same crystallographic orientation in the junction region. The lattice fringes are observed to have

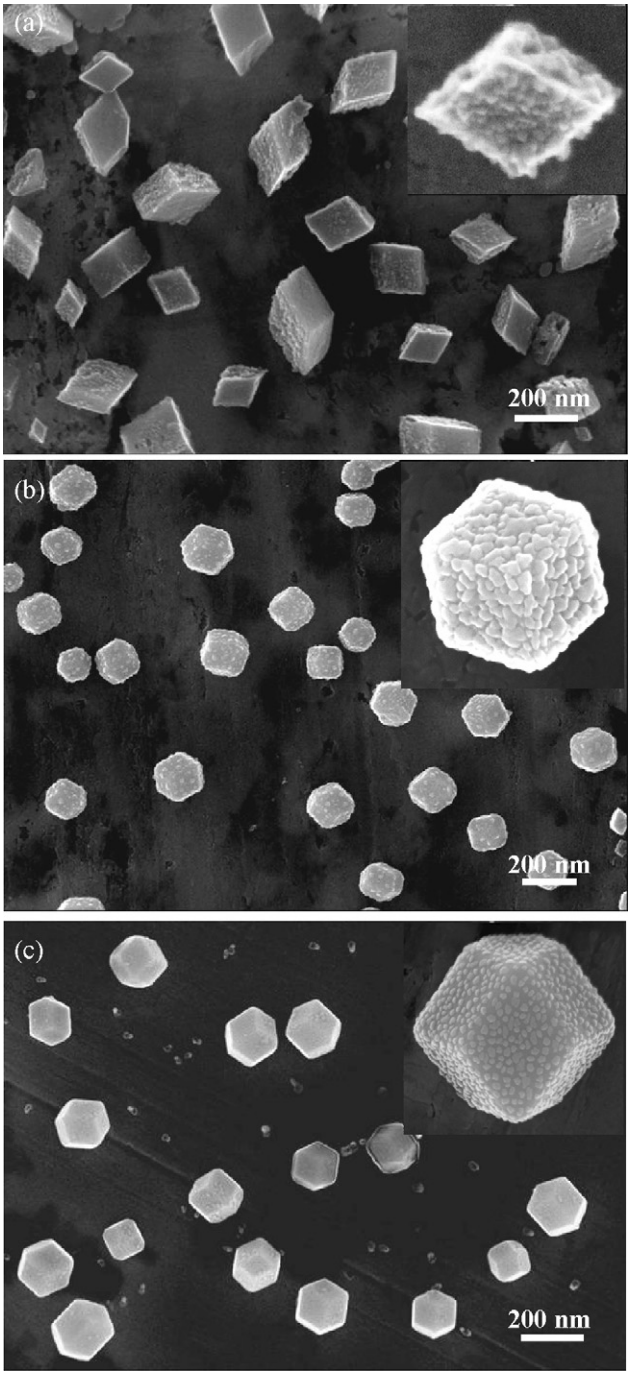

Figure 2 FESEM images of Ag_2O mesocrystals synthesized at silver ion concentration of 1 mM, applied potential and growth time of (a) rhombic hexahedron, 30 V @ 3 min, (b) cube, 15 V @ 3 min and (c) dodecahedron, 5 V @ 5 min.

a spacing of 0.238 nm corresponding to the interplanar spacing of (2 0 0) plane of Ag_2O, which is in good agreement with the XRD results (Fig. 1). The existence of mesopores (or defect, amorphous regions) during the assembly of the mesocrystal is clearly observed in the HRTEM image (dashed white circles in Fig. 3c) and the white spots in the TEM image in Fig. 3a and Fig. S2. The distinctive mesostructure consisting of mircopores or defect regions may be used to exploit the novel properties of the Ag_2O mesocrystals. E.g., microsensors, or microreactors, because these regions combining the rough surface may contribute to an enhanced reactivity [9].

In the applications of nanomaterials, apart from the shape effect, the size of nanostructures is another critical factor. In this study, the dependence of the mean size and the size distribution of the Ag_2O mesocrystals on the experimental conditions — applied potential, silver ion concentrations as well as the growth time — was investigated both in order to optimize the synthesis and to gain a better understanding of the formation of Ag_2O mesocrystals. Of these three parameters, the growth time plays the decisive role in the determination of the particle size. In order to get different shapes of Ag_2O mesocrystals, the applied potentials are adjusted as 30, 15 and 5 V, respectively. The silver ion concentrations are found to have significant influence on the dissolution of the Ag_2O (Fig. S3). At a high silver ion concentration, for example, 100 mM, due to low pH value, no Ag_2O product can be obtained. However, a lower silver ion concentration (e.g., <0.1 mM), results in a very low yield of Ag_2O dispersion. Therefore, in this study, a middle of silver ion concentration, 1 mM, is finally adopted. In Fig. 4a—c, the size evolutions of the Ag_2O mesocubes as a function of growth time are analyzed by SEM. The mean size of the Ag_2O mesocrystals can be adjusted from approximately 100 nm for the growth time of 2 min (Fig. 4a) to 200 nm for the growth

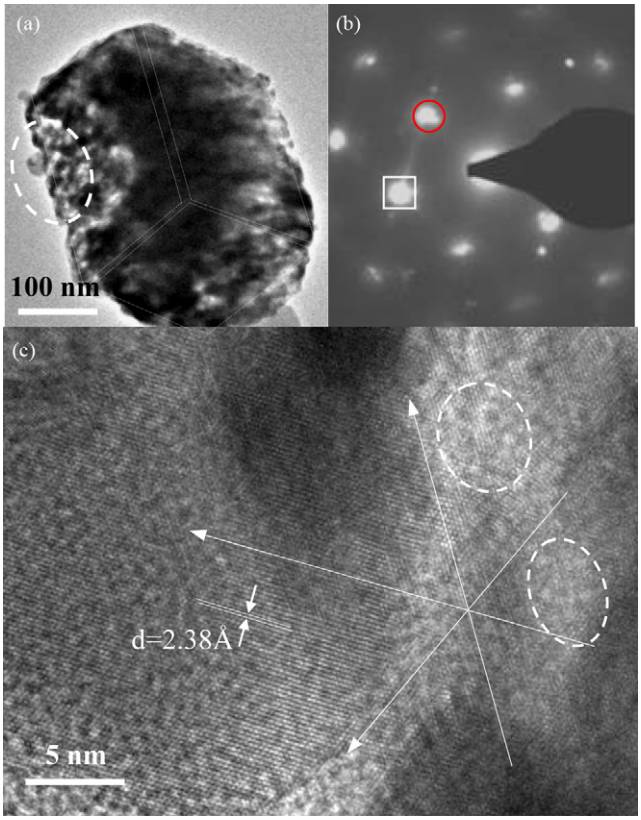

Figure 3 (a) TEM image of a single Ag_2O mesocube. (b) SAED pattern obtained from the whole Ag_2O mesocube, indicating the single crystal-like nature. The circled and boxed spots in the SAED pattern are indexed as {1 1 1} and {2 0 0} Bragg reflections. (c) HRTEM image taken from the dashed circle area of Fig. 2a. The white circles point to the mesopores and defects.

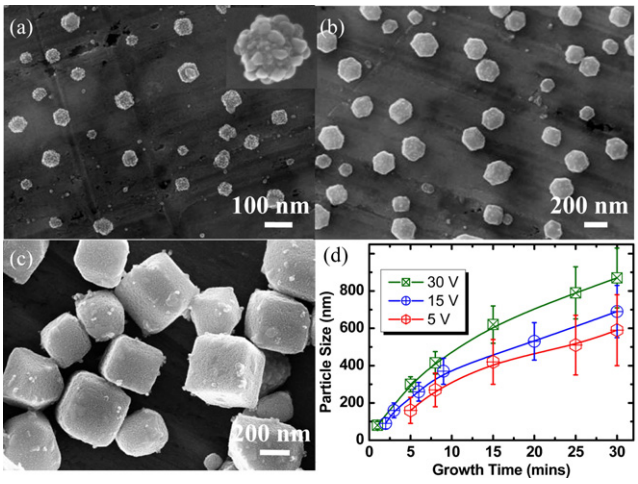

Figure 4 The FESEM images of Ag_2O mesocubes synthesized at an applied potential of 15 V and various growth time: (a) 1 min, (b) 5 min, (c) 30 min and (d) the average particle size versus growth time for various applied potentials.

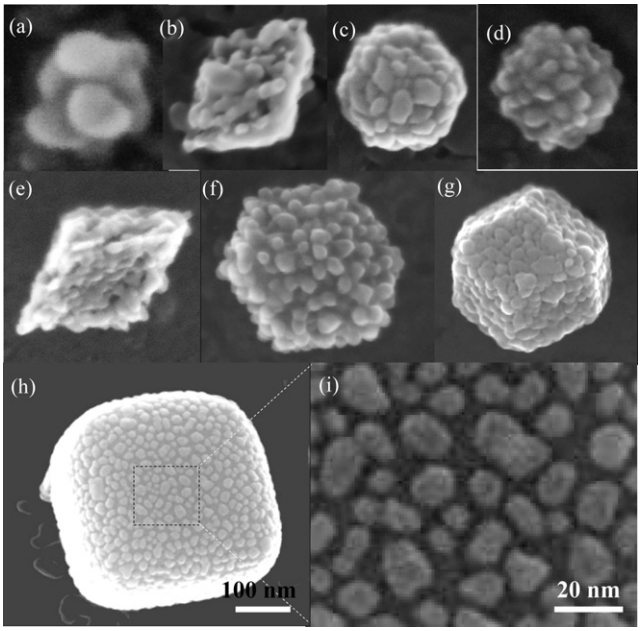

Figure 5 FESEM images of Ag_2O mesocrystals: (a) aggregate of Ag_2O nanoparticles, (b)—(d) typical quasi-polyhedral Ag_2O mesostructures with approximately 50 nm in size, (e)—(g) polyhedral Ag_2O mesocrystals with around 100 nm in size, (h) a typical Ag_2O mesocube with about 500 nm in size and (i) the high magnification image taken from the boxed area in Fig. 5h.

time of 5 min and to 600 nm for the growth time of 30 min. The growth-time dependence of mean size and size distributions for different shape of Ag_2O mesocrystals demonstrate the similar trend as shown in Fig. 4d. In general, the longer growth time, the larger Ag_2O mesocrystals may be synthesized. Meanwhile, the size distributions display a relatively larger standard deviation (the error bars in Fig. 4d).

Based on the above time-dependent size-evolution process, the detailed growth processes of Ag_2O mesocrystals can be explored, particularly at the early stage of the electrochemical reaction. It is noted that some small mesoscale particles of approximately 50 nm, e.g., the inset of Fig. 4a, have already shown the quasi-cube aggregates. This observation is supported by the SEM images in Fig. 5. In Fig. 5a, a small aggregate consists of quite a few primary particles (about 10 particles) for mesoscale assembly are demonstrated. As these aggregates grow to around 50 nm, the quasi-polyhedral shapes (rhombic hexahedron, cube and dodecahedron) can be frequently observed in the product as shown in Fig. 5b—d. With the further grow to approximately 100 nm, the well-defined polyhedral shapes are formed (Fig. 5e—g). After a longer time of electrochemical reaction, these Ag_2O mesocrystals still show a uniform shape owing to a relative stable silver ion concentration attributed to the sacrificial process of silver anode. For example, the Ag_2O mesocrystal (around 500 nm in size) grown under an applied potential of 15 V for a growth time of 20 min still displays the well-defined cubic shape as shown in Fig. 5h. It should be pointed out that, if we magnify the local region of this mesocube (Fig. 5h), a structure of Ag_2O primary particles embedded into Ag_2O matrix may be clearly observed (Fig. 5i). This suggests that, combining with the mesoscale assembly process (oriented attachment/rotation of building units), the crystallographic fusion or classical ion-mediated Ostwald ripening process could also occur. In other words, during the electrochemical reaction, even at the early stage of the oriented aggregation of the building units, the crystallographic fusion would immediately occur. However, whether the crystallographic fusion mentioned here is the same as the classical Ostwald ripening process has not been clarified clearly. In fact, the crystallographic fusion process or Ostwald ripening has been observed in various synthesis systems, e.g., in our previous study of the dendritic silver mesocrystals [17], the processes of mesoscale assembly and transformation with the assistance of Ostwald ripening was investigated. More recently, the similar Ostwald ripening process has also been found in the systems of CuO [8], $CaCO_3$ [35]. In the current study, a crystallographic fusion process of nanoparitlces rather than a dissolution—recrystallization (Ostwald ripening) mechanism can be suggested from the final porous nature (TEM images in Fig. 3a and c, and Fig. S2) of the mesocrystals, which would not occur upon redissolution—reprecipitation.

On the basis of these results, we propose a growth mechanism for the polyhedral structures of Ag_2O mesocrystals, which includes multiple different stages—the nucleation of building units, the oriented aggregations of the primary nanoparticles via an oriented attachment process, and the crystallographic fusion process. The schematic diagram is shown in Scheme 1. While, a key issue of the growth processes for the polyhedral structures of Ag_2O is how the primary nanoparticle units orderly aggregate and build up the ordered polyhedral meso-superstructures. This can be partly elucidated by the crystallographic surfaces that enclosed the crystals. In classical crystallization, the shape of crystals grown in solution is thermodynamically defined by minimizing the interface energies and the surface energies of all the exposed faces (Wulffs rule) [25,36]. This rule likely undergoes a generalization for both nanocrystal growth and mesocrystals assembly based on previous reports [27,35], including the formation of minimal surfaces in the initial nucleation stage and intermediately mutual ordering

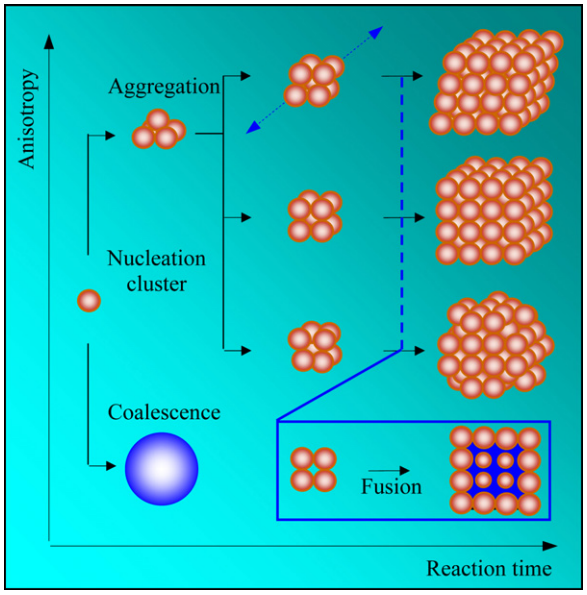

Scheme 1 The schematic illustration of the formation mechanism of Ag_2O mesocrystals and the overpotential-dependent shape-evolution processes.

(see also Figs. 3, 5 and S4). The process of oriented attachment, involving spontaneous self-organization of adjacent particles along a common crystallographic surface followed by joining of these particles at a planar interface, reduces overall energy by removing surface energy associated with unsatisfied bonds. The HRTEM images in Fig. S4a and b demonstrate that, in the initial nucleation stage, the nucleated primary nanoparticles can orderly attach each others. TEM image (Fig. S4c) and the corresponding SAED pattern (Fig. S4d) recorded from the small cube in Fig. S4c, indicate that the small mesocube has already had the tendency to orderly aggregate into a new mesostructure, although its size is only around 50 nm. These imply that, in the following coarsening process, the oriented attachment and rotation of building units can continuously proceed [37,38].

On the other hand, more importantly, the current electrochemical environment, serving as an external electric field, also rather critical to the mutual alignment of the nucleated Ag_2O building units and the mesoassembly in various polyhedral shape based on below experimental observations. In this study, in order to adjust the nucleation rate of the primary particles and the interaction forces between the primary particles under an external electric field, various overpotentials have been applied. Under a high-applied potential, an anisotropic assembly of the rhombic hexahedral Ag_2O mesocrystals can be achieved. If further increase of applied potential, e.g., 50 or 60 V (1 mM of silver ion concentration), some nanorods (Fig. S5) or nanowires (Fig. S6) of Ag_2O mesocrystals may be observed (see also Fig. 6a and b) due to the stronger anisotropic growth. On the contrary, under a medium high-applied potential, the product displays the isotropic shapes (cube or dodecahedron). If further decrease of the applied potential, e.g., to less than 2 V, some quasi-sphere nanoparticles result as shown in Fig. S7. However, it still follows a growth mode via the mesoscale assembly feature in this condition from the rough surface of the particles. When a relatively low potential is applied, e.g., the electrochemical reaction at 1 V and the silver ion concentration of 1 mM, the product shows the thermodynamically stable nanoparticles with smooth surface which are likely to grow via the classical ion-by-ion crystallization mode (Fig. 6c and d).

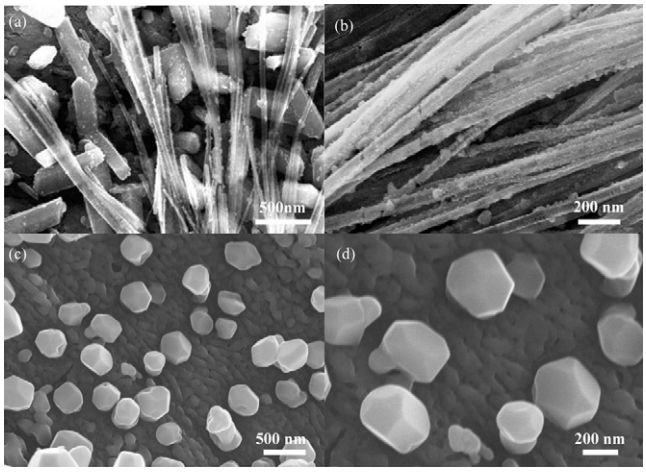

Figure 6 FESEM images of (a) and (b) Ag_2O mesostructures synthesized at silver ion concentration of 1 mM, applied potential and growth time of 60 V @ 10 min, and (c) and (d) Ag_2O nanostructures synthesized at SICs of 1 mM, applied potential and growth time of 1 V @ 10 min.

According to above overpotential-dependence shape- and structure-evolution as shown in Figs. 2, 6 and S5—S7, an external electric field is therefore very important to realize the ordering mesoassembly and tailor the shape of the Ag_2O meso-superstructures. In principle, all atoms and molecules are polarizable, for both polar and nonpolar atoms or molecules via coulombic interaction or van der Waals forces [39]. The polarized atoms or molecules may cause the dipole-dipole interactions and can also interact with an external electric/magnetic filed. In fact, previous studies have demonstrated that external electric fields can be used to create 2D and 3D superstructures for CdS nanorods [29] or CdSe nanorods [30] during the slow evaporation of the solvent. Recently, the influence of the intrinsic electric field on the biomimetic growth has been pointed out [40—42], and the external electric field has also been predicted to play an important role in the formation of highly ordered nanoparticle superstructures [32]. In this study, during electrochemical reaction, the nucleated Ag_2O building units may be also polarized to be dipoles. These dipoles can mutually attract each other in crystallographic register and aggregate into an ordered mesocrystal. At the same time, the interaction between these dipoles and the external electric field contribute to the anisotropic alignment, e.g., rhombic hexahedron, even mesorods or mesowires obtained at a relatively high overpotential.

Conclusions

We have presented, for the first time, an external electric field driven particle-mediated bottom-up approach that can be used to in situ build the Ag_2O meso-superstructures within an electrochemical deposition process. Different shapes

(rhombic hexahedron, cube and dodecahedron) and sizes (around 100 to ~800 nm) of Ag_2O mesocrystals have been obtained by the adjustment of the overpotential as well as the growth time. Various overpotentials play a crucial role in determining the shapes, structures as well as growth modes of the final product. The growth mechanism of polyhedral structures of Ag_2O mesocrystals is explained by the oriented attachment from the nature of crystallographic surfaces, and the external electric induced ordering alignment process of primary nanoparticle building units. Thus, the current strategy not only provides the direct evidence of an external electric field induced in situ mesoassembling process, but also may be extended to other systems to synthesize the mesostructures. In addition, the current protocol is highly scalable due to the high deposition speed which can be possible for the actual application.

Acknowledgments

We thank Dr. F. Schramm, and Dr. H. Jin, in Forschungszentrum Karlsruhe, Institut für Nanotechnologie, Germany, for their helpful discussions. J.X. Fang is grateful to Alexander-von-Humboldt Foundation for a fellowship to support his stay in Germany.

Appendix A. Supplementary data

Supplementary data associated with this article can be found, in the online version, at doi:10.1016/j.nantod.2010.05.002.

References

[1] H. Cölfen, S. Mann, Angew. Chem. Int. Ed. 42 (2003) 2350.
[2] M. Niederberger, H. Cölfen, Phys. Chem. Chem. Phys. 8 (2006) 3271.
[3] R. Lee Penn, J.F. Banfield, Science 281 (1998) 969.
[4] R.L. Penn, J.F. Banfield, Geochim. Cosmochim. Acta 63 (1999) 1549.
[5] G. Herrmann, H. Gleiter, G. Baro, Acta Metall. 24 (1976) 353.
[6] H. Cölfen, M. Antonietti, Angew. Chem. Int. Ed. 44 (2005) 5576.
[7] A.W. Xu, M. Antonietti, H. Cölfen, Y.P. Fang, Adv. Funct. Mater. 16 (2006) 903.
[8] X.D. Liang, L. Gao, S.W. Yang, J. Sun, Adv. Mater. 21 (2009) 2068.
[9] Z. Liu, X.D. Wen, X.L. Wu, Y.J. Gao, H.T. Chen, J. Zhu, P.K. Chu, J. Am. Chem. Soc. 131 (2009) 9405.
[10] L. Zhou, D.S. Boyle, P. O'Brien, J. Am. Chem. Soc. 130 (2008) 1309.
[11] I. Patla, S. Acharya, L. Zeiri, J. Israelachvili, S. Efrima, Y. Golan, Nano Lett. 7 (2007) 1459.
[12] P.T.K. Chin, J.W. Stouwdam, R.A.J. Janssen, Nano Lett. 9 (2009) 745.
[13] A.N. Kulak, P. Iddon, Y. Li, S.P. Armes, H. Cölfen, O. Paris, R.M. Wilson, F.C. Meldrum, J. Am. Chem. Soc. 129 (2007) 3729.
[14] J.X. Fang, X.N. Ma, H.H. Cai, X.P. Song, B.J. Ding, Nanotechology 17 (2006) 5841.
[15] J.X. Fang, H.J. You, P. Kong, Y. Yi, X.P. Song, B.J. Ding, Crys. Growth Des. 7 (2007) 864.
[16] J.X. Fang, B.J. Ding, X.P. Song, Cryst. Growth Des. 8 (2008) 3616.
[17] J.X. Fang, B.J. Ding, X.P. Song, Y. Han, Appl. Phys. Lett. 92 (2008) 173120.
[18] Y.G. Sun, Y.N. Xia, Science 298 (2002) 2176.
[19] S.a. Beccara, G. Dalba, P. Fornasini, R. Grisenti, A. Sanson, Phys. Rev. Lett. 89 (2002) 025503.
[20] M. Bielmann, P. Schwaller, P. Ruffieux, O. Gröning, L. Schlapbach, P. Gröning, Phys. Rev. B 65 (2002) 235431.
[21] Y. Ida, S. Watase, T. Shinagawa, M. Watanabe, M. Chigane, M. Inaba, A. Tasaka, M. Izaki, Chem. Mater. 20 (2008) 1254.
[22] J. Ghilane, F.R.F. Fan, A.J. Bard, Nano Lett. 7 (2007) 406.
[23] D. Dellasega, A. Facibeni, F.Di. Fonzo, M. Bogana, A. Polissi, C. Conti, C. Ducati, C.S. Casari, A.L. Bassi, C.E. Bottani, Nanotechnology 19 (2008) 475602.
[24] Y.J. Xiong, B.J. Wiley, Y.N. Xia, Angew. Chem. Int. Ed. 46 (2007) 2.
[25] Z.L. Wang, J. Phys. Chem. B 104 (2000) 1153.
[26] M.J. Siegfried, K.S. Choi, J. Am. Chem. Soc. 128 (2006) 10356.
[27] X.W. Wei, G.X. Zhu, Y.J. Liu, Y.H. Ni, Y. Song, Z. Xu, Chem. Mater. 20 (2008) 6248.
[28] A. Ahniyaz, Y. Sakamoto, L. Bergström, PNAS 104 (2007) 17570.
[29] K.M. Ryan, A. Mastroianni, K.A. Stancil, H.T. Liu, A.P. Alivisatos, Nano Lett. 7 (2006) 1479.
[30] S. Gupta, Q.L. Zhang, T. Emrick, T.P. Russell, Nano Lett. 9 (2006) 2066.
[31] R.Q. Song, H. Cölfen, Adv. Mater. 22 (2009) 1301.
[32] T. Wang, H. Cölfen, M. Antonietti, Chem. Eur. J. 12 (2006) 5722.
[33] J.X. Fang, H. Hahn, R. Krupke, F. Schramm, T. Scherer, B.J. Ding, X.P. Song, Chem. Commun. (2009) 1130.
[34] M.T. Reetz, W. Helbig, J. Am. Chem. Soc. 116 (1994) 7401.
[35] R.Q. Song, A.W. Xu, M. Antonietti, H. Cölfen, Angew. Chem. Int. Ed. 48 (2009) 395.
[36] G. Wullf, Z. Kristallogr. 34 (1901) 449.
[37] Z.H. Yu, M.A. Hahn, S.E. Maccagnano-Zacher, J. Calcines, T.D. Krauss, E.S. Alldredge, H. Silcox, ACS Nano 2 (2008) 1179.
[38] Y. Lu, J.Y. Huang, C. Wang, S.H. Sun, J. Lou, Nat. Nanotechnol. 5 (2010) 218.
[39] D. Myers, Surfaces, Interfaces, and Colloids: Principles and Applications, John Wiley, 1999.
[40] S. Busch, H. Dolhaine, A. DuChesne, S. Heinz, O. Hochrein, F. Laeri, O. Podebrad, U. Vietze, T. Weiland, R. Kniep, Eur. J. Inorg. Chem. (1999) 1643.
[41] P. Simon, D. Zahn, H. Lichte, R. Kniep, Angew. Chem. Int. Ed. 45 (2006) 1911.
[42] P. Simon, E. Rosseeva, J. Buder, W. Carrillo-Cabrera, R. Kniep, Adv. Funct. Mater. 19 (2009) 3596.

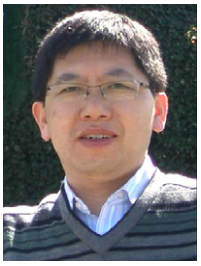

Jixiang Fang was born in LiaoNing (China) in 1976. In 2007, he received his PhD in Materials Science in Xi'an Jiaotong University. In 2008, he spent 1 year in his post-doctorate stage at Institute of Nanotechnology (INT), Karlsruhe Institute of Technology (KIT). Since 2009, He is working as Alexander-von-Humboldt scholar with Prof. Herbert Gleiter in INT (KIT). His research has involved crystal growth, electrochemical deposition, nanoglasses for optical and mechanical application.

Philipp M. Leufke was born in Freiburg (Germany) in 1981 and studied physics at the University of Constance (Germany), where he received his diploma degree in 2007. He is currently working on his PhD thesis at the University of Darmstadt and Institute of Nanotechnology (INT), Insititute of Technology (KIT). His scientific interests include magnetic and conductive oxide thin films grown by means of ultra-high vacuum (UHV) techniques.

Robert Kruk was born in Przemysl (Poland) and in 1989 he received his Master's degree in Physics at Jagellonian University, Krakow. In 1995 he received his PhD degree in Physics at Jagellonian University, Krakow. He spent 3 years (1999—2002) as a research associate at Northern Illinois University, USA. Since 2007 he has been working as a research scientist at Institute of Nanotechnology, Karlsruhe Institute of Technology, Germany. His research interests and expertise include: Electronic structure and magnetic properties of intermetallic compounds with uranium and rare earth metals; strongly correlated systems with focus on electronic and magnetic properties; reversible control of the electronic transport in conducting oxide nanostructures; electrostatic modulation (electrostatic doping) of the carrier density of materials other than conventional semiconductors; such as metals, metallic-like oxides and strongly correlated oxides.

Di Wang received his PhD degree in Institute of Physics, Chinese Academy of Sciences in 2001. From 2001 to 2009, he worked in Fritz Haber Institute of Max-Planck-Society, Berlin (Germany). During this period, he mainly worked in the fields of TEM characterization of heterogeneous catalysts. From May of 2009, he started to work in Institute of Nanotechnology, Karlsruhe Institute of Technology. His scientific interests include new technology and instrumentation in TEM, like aberration corrected TEM, applications of TEM and related techniques on nano-structured materials and other advanced materials, and image processing methods.

Horst Hahn studied Materials Science at the Universitat des Saarlandes and received his PhD from the Technische Universitat Berlin. He was a post-doctoral fellow at the Universitat des Saarlandes working in the area of interfaces and nanocrystalline metals. From 1985 to 1987 Dr. Hahn was a Research Associate in the Materials Science Division at Argonne National Laboratory where he established a research program on nanocrystalline ceramics. Subsequently, he was Research Assistant Professor in the Materials Research Laboratory at the University of Illinois at Urbana-Champaign for 2 years. In 1992 he became Associate Professor of Materials Science at Turgers—The State University of New Jersey. From 1992 to 2004 Horst Hahn was Full Professor (C4) in the Department of Materials Science at Technische Universitat Darmstadt and Head of the Thin Films Division. Since April 2004 Professor Horst Hahn is Managing Director of the Institute for Nanotechnology at the Forschungszentrum Karlsruhe and Director of the Research Laboratory Nanomaterials located at the Technische Universitat Darmstadt and jointly operated by Forschungszentrum Karlsruhe and Technische Universitat Darmstadt.